Thermoluminescence mechanism in CdF_2:Eu

H. Przybylińska and M. Godlewski
Institute of Physics, Polish Academy of Sciences, 02-668 Warsaw, Poland

D. Hommel
Physikalisches Institut der Universität Würzburg, Am Hubland, D-8700 Würzburg, Germany
(Received 4 October 1991)

A model explaining all the features of the complex thermoluminescence (TL) process in CdF_2:Eu is presented, based on extensive optical and EPR studies. It is shown that two types of europium centers are active in the TL process: the charge-compensated Eu^{3+}-O_s^{2-} or Eu^{3+}-F_i^- complexes (the centers dominating the photoluminescence under uv excitation), which act as the source of electrons as well as recombination centers, and the Eu^{3+} centers with cubic site symmetry, which are the electron traps. The TL excitation proceeds via the allowed intra-impurity transition of the fluorine (oxygen) coactivator, and the electrons are autoionized from the coactivator excited states through a lattice-relaxation-induced potential barrier. The different barriers for electron recapture by the ionized fluorine and oxygen coactivators are shown to be responsible for the different activation energies observed in the thermoluminescence of Eu^{3+}-O_s^{2-} and Eu^{3+}-F_i^- centers.

I. INTRODUCTION

The continuous interest in the studies of rare-earth activated wide band-gap compounds is stimulated by their various possible applications. For example, such compounds as $CaSO_4$ can be widely used in thermoluminescence (TL) dosimetry. It was shown that the TL response of $CaSO_4$:Eu to uv radiation is several orders of magnitude greater than that of any other related material.[1] The extremely bright thermoluminescence[2] observed by us in CdF_2:Eu has, therefore, attracted our interest. In this paper we present a comprehensive study of the thermoluminescence processes in CdF_2:Eu.

The nature of the complex photoluminescence (PL) in CdF_2:Eu has been studied in detail by many authors, see, e.g., Refs. 3–5. The general outcome of all these studies is that a whole range of different Eu^{3+} centers, by which we mean Eu^{3+} ions with different local site symmetries, are active in the PL. For example, in the studies of Sun-Il Mho and Wright[5] 17 different Eu^{3+} centers have been observed. The reason for the occurrence of such a large number of centers is that the additional positive charge of Eu^{3+} (which substitutes the Cd^{2+} ion in the lattice) requires charge compensation, which can be different depending on sample preparation. Typically, europium is introduced as EuF_3 or Eu_2O_3 and the charge compensation is realized then mainly by interstitial fluorine ions (F_i^-) or by substitutional oxygen ions (O_s^{2-}), respectively. In the case when the compensating ions are located close to Eu^{3+}, i.e., oxygen is at the nearest anion site in the [111] direction and fluorine is at the nearest interstitial position in the [100] direction, the so-called C_{3v} and C_{4v} centers of Eu^{3+} are formed. These two types of centers together with the C_{2v} center, which consists of a Eu^{3+}-Eu^{3+} pair with two close-lying interstitial fluorine ions, play a dominant role in the PL in our crystals. What distinguishes the C_{3v} and C_{4v} centers from the other centers observed is that they are most efficiently excited via broad bands in the uv region, whereas other Eu^{3+} associates require site-selective excitation. The broad-band excitation process for C_{3v} centers has been previously studied by one of the authors.[3] It was found that the uv illumination induces the allowed $2p \rightarrow 3s$ transition ($^1S_0 \rightarrow {}^1P_1$) within the coactivator O_s^{2-} (or F_i^-) and the excitation energy is then transferred to the Eu^{3+} ion resulting in Eu^{3+} radiative deexcitation. These facts are recalled here because, as it will be shown, the thermoluminescence in our crystals is dominated by the emissions of C_{3v} and C_{4v} centers.

Since in the TL process the optically induced electrons are stored at excited metastable states and the process of their release is thermally activated, it should be first of all determined whether the TL process is localized and some metastable excited state of the Eu^{3+}-coactivator pair is involved, or nonlocalized, i.e., the Eu^{3+}-coactivator pairs are ionized. In the latter case the nature of the electron trap and the mechanism of the thermally activated deexcitation process should be established. These problems will be discussed in Sec. IV. We will show that the TL process in CdF_2:Eu is activated by charge-transfer processes from PL active C_{3v} and C_{4v} Eu^{3+} complexes to isolated Eu^{3+} centers forming Eu^{2+} donor states in the CdF_2 lattice.

We acknowledge here the previous attempts to solve the above-listed problems.[6–11] However, despite intensive studies the mechanism of the CdF_2:Eu TL has remained unclear. Though most of the results seem to point to a nonlocalized process, with the Eu^{2+} donor being the electron trap, the activation energies of the TL were larger than the Eu^{2+} activation enthalpy. The second difficulty was the understanding of the TL excitation process.

II. EXPERIMENT

The Eu^{3+} PL was excited with a high-pressure mercury lamp and a double-quartz monochromator. The PL and TL spectra were measured using a GDM 1000 monochromator, a Hamamatsu cooled photomultiplier, and a lock-in amplifier. The excitation spectra were recorded in the same experimental setup but using a high-pressure xenon lamp. To measure the TL glow curves the samples were illuminated at 100 K and then heated up to room temperature with the rate of 0.011 K/s. The absorption was measured in the range 0.2–20 μm with use of Carl-Zeiss-Jena IR and UV-VIS specords, Cary 17 and Hitachi-Perkin-Elmer spectrometers.

The EPR measurements were performed on a standard BRUKER X-band spectrometer. A high-pressure xenon lamp, monochromator, and a set of Carl-Zeiss Jena interference filters were used for sample illumination.

The crystals were grown by the Bridgman-Stockbarger method from powdered CdF_2 purified by several zone-melting runs and mixed with 1 mol% and 0.1 mol% of EuF_3 or Eu_2O_3. Some of the samples were additionally annealed in F_2 or O_2 vapor at 500 °C to increase the concentration of C_{4v} and C_{3v} centers, respectively. Conversion from the 3+ to 2+ charge state of Eu was obtained by annealing the crystals in H_2 atmosphere at temperatures between 300 °C and 600 °C for a few minutes up to 1 h depending on the desired level of conversion.

III. RESULTS

Detailed PL studies revealed that the as-grown samples contained Eu^{3+} centers of C_{2v} symmetry (Eu^{3+}-Eu^{3+} pairs compensated by two close-lying interstitial fluorine ions), centers of C_{3v} symmetry (Eu^{3+} compensated by an oxygen ion replacing one of the nearest-neighbor fluorine ligands), and centers of C_{4v} symmetry (Eu^{3+} compensated by a fluorine ion at the nearest interstitial site). A weak PL spectrum of isolated Eu^{3+} centers (O_h symmetry) could be also observed. The relative concentrations of these centers depend on the sample preparation. The type of center which dominates in the PL could be changed by first converting the crystal and then annealing in F_2 or O_2 atmosphere (to obtain C_{4v} or C_{3v} centers, respectively). For illustration the PL spectra corresponding to the strong $^5D_0 \rightarrow {}^7F_1$ magnetic dipole transition of Eu^{3+} for all four symmetries, as measured for the as-grown 1 mol% Eu sample, are shown in Fig. 1(a). The figure shows collected data as the centers have different excitation spectra and, in principle, cannot be all observed simultaneously. The number of lines observed for a given symmetry reflects the crystal-field splitting of the $^7F_1$ state. For the cubic symmetry the $^7F_1$ state is unsplit whereas for the lowest C_{2v} symmetry the degeneracy is totally lifted. For the C_{4v} and C_{3v} centers the $^7F_1$ state splits into a singlet A_2 and a doublet E. The transition to the E doublet for C_{3v} centers occurs at a lower energy

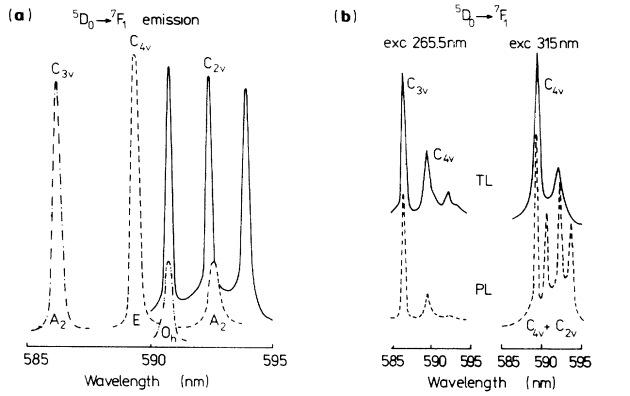

FIG. 1. (a) Collected PL spectra corresponding to the strong $^5D_0 \rightarrow {}^7F_i$ transition of Eu^{3+} in the as-grown CdF_2:Eu 1 mol% sample. The emission lines attributed to Eu^{3+} centers of C_{2v}, C_{3v}, C_{4v}, and O_h symmetries are marked. (b) PL (dashed line) and TL (solid line) spectra observed in the same sample under 265.5-nm (left) and 315-nm excitations.

(16 692 cm^{-1}) and is not shown in the figure.

The C_{2v} and O_h centers are excited only by narrow lines corresponding to the intrashell transitions of Eu^{3+}, whereas the most efficient excitation of the C_{3v} and C_{4v} centers proceeds via broad, Gaussian-shaped bands in the uv region with the maxima at 254 nm (4.88 eV) and 286 nm (4.34 eV), respectively. The same bands can be also observed in the absorption spectra of samples with high concentrations of C_{3v} and C_{4v} centers, and have been shown to be due to allowed $2p \rightarrow 3s$ transitions of the O_s^{2-} (254 nm) and F_i^- (286 nm) coactivators.[3] In Fig. 2 the absorption and excitation spectra for C_{4v} and C_{3v} centers are shown. The measurements have been performed on samples annealed in fluorine and oxygen vapor, respectively.

In the TL spectra only the emission of C_{3v} and C_{4v} centers was observed. The brightest TL was obtained in the as-grown CdF_2:Eu 1% sample. The TL spectra induced by two different illuminations (265.5 and 315 nm) are shown in Fig. 1(b) and compared to the PL spectra observed under the same excitation. It can be seen that no emission of C_{2v} centers is observed in the TL though it dominates in the PL spectrum. Moreover, the relative intensities of the C_{4v} and C_{3v} emissions are different in TL and PL.

To clear up the mechanism of energy storage leading to TL we measured the CdF_2 absorption before and after 15 min of uv excitation at 77 K. We employed a Hitachi-Perkin-Elmer spectrometer with a memory system which allows to measure very small absorption changes. The uv-light-induced changes of the absorption spectra are shown in Fig. 3 for two CdF_2:Eu 0.1% samples, which were additionally annealed in oxygen but for different periods. Before the treatment both samples contained mainly C_{4v} centers. After long annealing practically only C_{3v} centers are present in the sample (Fig. 3 left-hand side), whereas the sample lightly annealed in oxygen contains both C_{4v} and C_{3v} centers (right-hand side). It can

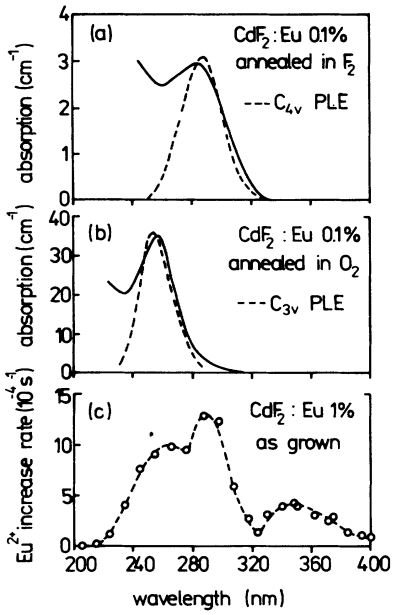

FIG. 2. The absorption (solid lines) and PL excitation (dashed lines) spectra of (a) C_{4v} and (b) C_{3v} centers measured in CdF_2:Eu 0.1% crystals annealed in (a) fluorine and (b) oxygen vapor. (c) The spectral dependence of the increase rate, τ_i^{-1}, of the Eu^{2+} EPR signal intensity under illumination measured in the as-grown CdF_2:Eu 1 mol% sample. The data have been corrected for constant light intensity.

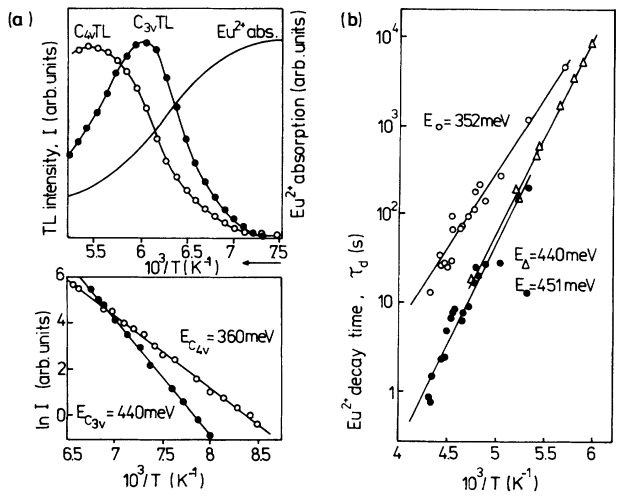

FIG. 4. (a) Top: temperature dependence of the Eu^{2+} absorption coefficient (solid line) and the TL glow curves of C_{3v} (full circles) and C_{4v} (open circles) centers. Bottom: evaluation of the TL activation energies. (b) The temperature dependencies of the decay times τ_d of the fast (full circles) and slow (open circles) components of the Eu^{2+} signal decay observed after the broadband uv illumination was turned off, as well as of the decay after the 254-nm excitation was turned off (triangles).

be seen that uv illumination leads to a decrease in the intensity of the coactivator absorption bands and to the appearance of an additional band, which is due to the $4f^7 \rightarrow 4f^6 5d^1$ transition of Eu^{2+}. The population of Eu^{2+} states is metastable and decreases with increasing temperature, while the TL intensity increases. The temperature dependence of the Eu^{2+} absorption is shown in Fig. 4(a) together with the TL glow curves for C_{3v} and C_{4v} centers, which were found to be slightly different. The activation energies obtained from the TL increase at low temperatures are 360±15 and 440±15 meV, respectively. It was found, moreover, that very long annealing, either in O_2 or in F_2 vapor, leads to a decrease of the efficiencies of both the TL and the $Eu^{3+} \rightarrow Eu^{2+}$ photoconversion processes.

In all the samples in which TL was observed an EPR spectrum of Eu^{2+} was detected after illumination of the sample with uv light at low temperature. The same spectrum was observed in crystals converted by annealing in Cd or H_2 vapor. It consists of seven groups of lines, arising from the allowed $\Delta M = 1$ transitions within the $^8S_{7/2}$ ground multiplet of Eu^{2+}, with a rich hyperfine structure due to Eu^{151} and Eu^{153} isotopes with the natural abundances of 47.77% and 52.23%, respectively, both having a nuclear spin of $I = \frac{5}{2}$. The angular dependence of this spectrum was measured and is shown in Fig. 5 for the

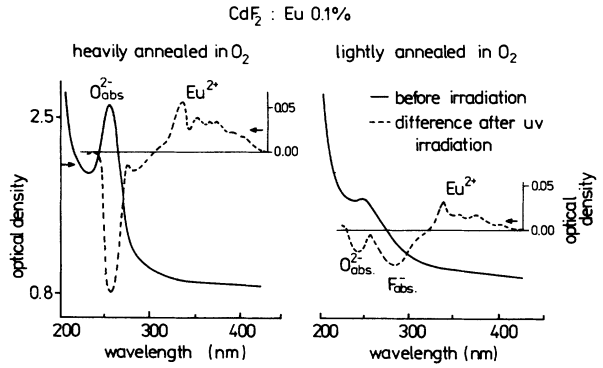

FIG. 3. The absorption spectrum before illumination (solid line), and the absorption changes after 15 min of uv illumination at 77 K (dashed line) for two CdF_2:EuF_3 0.1 mol% samples heavily (left-hand side) and lightly (right-hand side) annealed in oxygen.

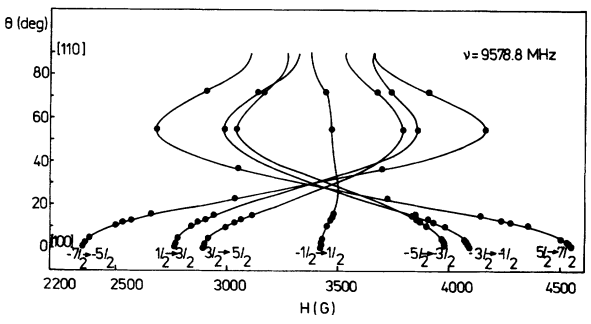

FIG. 5. The angular dependence of uv-light-induced EPR spectrum of Eu^{2+} for the magnetic field rotated in the (110) plane. For the sake of simplicity only the center of gravity of each set of the 12 observed hyperfine structure lines is marked. The solid line represents the values calculated with use of the spin-Hamiltonian parameters given in Table I.

magnetic field rotated in the (110) plane.

In the CdF_2:Eu 1 mol% sample, characterized by the brightest thermoluminescence, a weak EPR signal of Eu^{2+} was observed prior to illumination. The intensity of this signal was found to increase under illumination with uv light at temperatures below 230 K. The maximal concentration of photogenerated Eu^{2+} centers was $(1.6\pm0.4)\times10^{17}$ cm^{-3} and was reached for temperatures below 160 K. In this temperature region the occupancy of Eu^{2+} states was found to be metastable (no decrease of the signal intensity was observed after the light had been turned off). The kinetics of the EPR signal increase under illumination were measured for various wavelengths of the incident light at 130 K. The increase rate τ_i^{-1} of the Eu^{2+} EPR signal intensity was determined from the initial rise of the kinetics and normalized to constant light intensity making use of the observed linear dependence of the increase rate on light intensity. As can be seen in Fig. 2(c) the Eu^{2+} photogeneration spectrum, $\tau_i^{-1}(\lambda)$, consists of two bands superimposed on each other, having the maxima at 288 and 254 nm. These bands correspond exactly to the PL excitation spectra of C_{4v} and C_{3v} centers, respectively. The relative intensities of these two bands were found to depend on temperature. As it turned out the increase rate of the Eu^{2+} EPR signal has a different temperature dependence for light energies from the C_{4v} and C_{3v} excitation regions.

The kinetics of Eu^{2+} photogeneration were measured as a function of temperature for two different illuminations coinciding with the excitation of C_{4v} centers (300 nm) and C_{3v} centers (254 nm). The temperature range was chosen so that no thermal depopulation of Eu^{2+} centers was taking place. The temperature dependence of the increase rates (determined from the initial rise of each kinetics) is shown in Fig. 6. The open and full circles denote the experimental values obtained for the 300- and 254-nm excitations, respectively. It can be seen that for both illuminations the increase rate has a thermally activated character, however, the activation energies are different and equal to 13 ± 2 meV for the light energy from the C_{4v} PL excitation region and 56 ± 7 meV for the C_{3v} excitation. This implies that the ionization processes of F_i^- and O_s^{2-} coactivators are thermally activated with different activation energies.

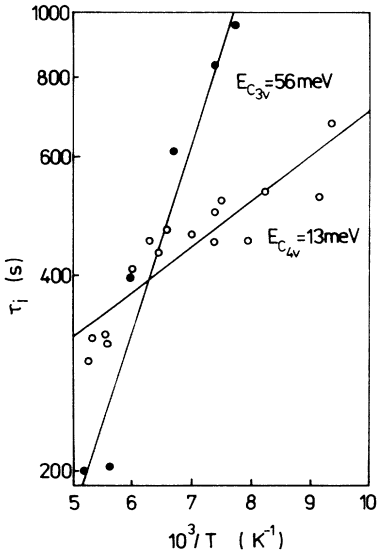

FIG. 6. The temperature dependence of the increase rate of the Eu^{2+} EPR signal intensity for two different excitations: 300 nm (open circles) and 254 nm (full circles).

At temperatures above 160 K the occupancy of light-induced Eu^{2+} centers is no longer metastable and a slow decrease of the EPR signal intensity is observed after the light is turned off. It was found that after a broadband uv excitation the kinetics of the EPR signal decrease consisted of a sum of two exponential decays: a "fast" one, the contribution of which increases with increasing temperature, and a "slow" one. The temperature dependencies of the decay times τ_d of the fast (full circles) and slow (open circles) components of the decrease are shown in Fig. 4(b). The two components are found to be exponentially dependent on temperature but are characterized by different activation energies: 451 ± 28 meV for the fast component and 352 ± 17 meV for the slow one. This indicates the existence of two different recombination centers and is consistent with the results of TL measurements. The two activation energies observed in the thermal depopulation of Eu^{2+} centers are close to the TL activation energies of C_{3v} (440 ± 15 meV) and C_{4v} (360 ± 15 meV) centers. When a selective excitation was used the kinetics of Eu^{2+} EPR signal decrease after the light was turned off showed a single-exponential behavior. The temperature dependence of the decay time after 254-nm excitation is shown in Fig. 4(b) (triangles). The decay time as well as the activation energy of this decay (440 ± 17 meV) are comparable to those of the fast component observed when a broadband excitation was applied.

IV. DISCUSSION

A. The nature of the thermoluminescence emission

As it is demonstrated in Fig. 1(b) the TL spectra are dominated by the emissions of C_{3v} and C_{4v} centers, those excited via coactivators. There is no emission of C_{2v} centers, though they are found to be the dominant centers in PL measured under the same excitation (the 315.5-nm excitation applied coincides with the $^7F_J \rightarrow {}^5H_6$ intrashell transition of Eu^{3+} in C_{2v} symmetry[11]). This fact indicates that the O_s^{2-} and F_i^- coactivators may play a decisive role in the TL process.

Figure 1(b) proves that the radiative deexcitation of C_{3v} and C_{4v} centers in both the TL and PL processes is identical, except that in the case of TL the radiative deexcitation process is thermally activated. On the other hand the results depicted in Fig. 3 show directly that after illumination with uv light at low temperature the intensities of the O_s^{2-} and F_i^- absorption bands are reduced and an absorption band appears,[12] which is due to the $4f^7 \rightarrow 4f^6 5d^1$ transition of Eu^{2+}. This proves that during uv illumination oxygen and fluorine coactivators are ionized and the electrons are trapped by Eu^{3+}

centers. At first view, this result seems to contradict earlier findings. It was previously shown that the broad, Gaussian-shaped band with the maximum at 254 nm is due to the internal $2p^6 \rightarrow 2p^5 3s^1$ transition of the oxygen coactivator, and does not have a photoionizing character.[3] Moreover, it was shown that recombination from the excited $2p^5 3s^1$ state results in very efficient energy transfer to Eu^{3+} within the C_{3v} complex. Now, it appears that the same transition induces free electrons which populate the Eu^{2+} centers. The only possible explanation of this puzzle is the possibility of ionization (autoionization) of the excited state of the coactivator, which would require its location close to the continuum of the conduction-band states. This model will be further confirmed in the following sections of this paper.

As can be seen in Fig. 4(a) the TL process and the population of the Eu^{2+} state are correlated. This opens the fundamental question what is the nature of the Eu^{3+} states which capture the electrons, are they isolated "cubic" Eu^{3+} centers or those constituting the Eu^{3+}-coactivator pair. Some of the experimental results seem to point to the latter possibility. The TL activation energies of C_{4v} and C_{3v} centers are different and larger than the activation energy of the conductivity in chemically converted CdF_2:Eu crystals (which contain cubic Eu^{2+} centers). This might be explained by the presence of close-lying coactivator ions disturbing the activation enthalpy of Eu^{2+}. Therefore, before further discussion of the TL nature the local symmetry of Eu^{2+} ions has to be determined. To this end we employed the EPR technique. The analysis of the EPR spectrum of the light-induced Eu^{2+} centers is presented in Sec. IV B.

B. The nature of the electron trap

Europium ions in CdF_2 can be incorporated in two charge states, Eu^{3+} and Eu^{2+}. The ground state of Eu^{3+}, $^7F_0$, is diamagnetic and cannot be studied by means of the EPR technique. It is not the case for Eu^{2+}, for which the ground state ($^8S_{7/2}$) is easily observed. The EPR spectrum of Eu^{2+} observed in our crystals after excitation with uv light is identical to the one observed after thermal conversion and agrees well with the spectrum reported previously[13,14] for cubic Eu^{2+} centers in CdF_2. The experimental results are well described with the spin Hamiltonian for a $^8S_{7/2}$ octet ($S=\frac{7}{2}$) in a crystal field of cubic symmetry:

$$H_S = g\beta \bar{S}\,\bar{B} + \tfrac{1}{60} b_4 (O_4^0 + 5\,O_4^4) + \tfrac{1}{1260} b_6 (O_6^0 - 21\,O_6^4) + \sum_i A_i \bar{S}\,\bar{I}\,,$$

where g is the isotropic g factor, β is the Bohr magneton, A_i ($i=151,153$) are the hyperfine structure constants of the two Eu^{151} and Eu^{153} isotopes, and the two terms with b_4 and b_6 constants are the crystal-field terms. The parameters obtained from the fit of the above spin Hamiltonian to the experimental spectrum are summarized in Table I. For comparison the spin-Hamiltonian parameters as derived from previous studies[14–16] are also given. Moreover, there is a perfect agreement of the measured angular dependence of the spectrum with the one calculated using the same parameters and the formulas given by Lacroix[17] (see Fig. 5). All this proves that the Eu^{2+} centers populated during uv excitation are isolated substitutional europium ions well separated from the F_i^- and O_s^{2-} coactivators.

This conclusion explains why only a small fraction (approximately 1%) of the C_{3v} and C_{4v} sites observed in the PL measurements were found to be active in TL. The TL efficiency is limited by the concentration of cubic (O_h) Eu^{3+} centers acting as electron trap. This fact could not be understood in the case of an intrasite charge transfer.

C. The activation enthalpy of the Eu^{2+} electron trap

In order to construct the model of the thermoluminescence process the activation enthalpy (thermal-ionization energy at $T=0$ K) of the electron trap should be known. It has been previously found that after thermal conversion the CdF_2:Eu crystals are conducting, with the dc conductivity characterized by a 330-meV activation energy.[18] However, since only the conductivity has been measured the exact value of the Eu^{2+} activation enthalpy remained unknown. This is because the transport mechanism in the CdF_2 lattice is still not clear. The same difficulty will arise when discussing the emission and capture processes. The problem of appropriate descriptions of the $\sigma_{dc}(T)$ dependence for different conductivity mechanisms is discussed, e.g., in Ref. 19.

The EPR technique would provide, apparently, a simple method to determine the ionization enthalpy of Eu^{2+}, by studying the temperature dependence of the Eu^{2+} EPR signal intensity, which is directly proportional to the concentration of Eu^{2+} centers. In conducting samples, however, the thermal depopulation of a center affects the signal intensity in two ways: directly, and indirectly—by effectively changing the sample volume penetrated by microwave radiation due to the increase of conductivity (the so-called skin effect). As it turns out, even in samples with relatively low Eu^{2+} concentration (10^{17} cm^{-3}) both these effects are of the same order of

TABLE I. Spin-Hamiltonian parameters for Eu^{2+} in CdF_2.

T (K)	g factor	b_4 (10^{-4} cm^{-1})	b_6 (10^{-4} cm^{-1})	A_{151} (10^{-4} cm^{-1})	A_{153} (10^{-4} cm^{-1})	Ref.
280	1.9918±0.0005	−51.4±0.5	0.24±0.2	−33.9±0.2	−15.0±0.2	this work
300	1.9918±0.0005	−52.37±0.1	0.24±0.05	−33.9±0.15	−15.05±0.15	Ref. 14
77	1.9923±0.0006	−56.04±0.15	0.28±0.1	−34.15±0.15	−15.15±0.15	Ref. 14
300	1.9885±0.001	±51.94±0.5				Ref. 15
				−34.2153±0.0007	−15.1865±0.0007	ENDOR data (Ref. 16)

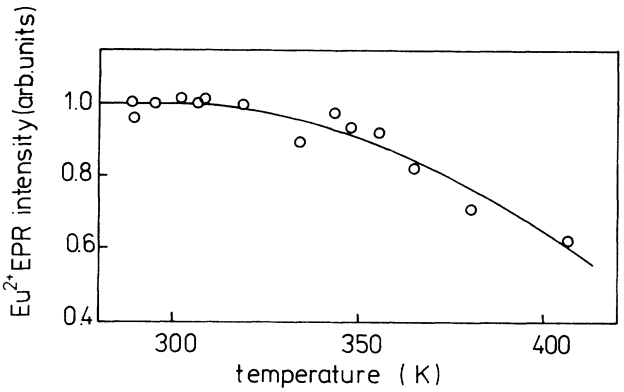

FIG. 7. The temperature dependence of the Eu^{2+} EPR signal intensity in the CdF_2:Eu 1% sample (without illumination). Eu^{2+} concentration at 250 K was 1.3×10^{17} cm^{-3}. The solid line is the calculated dependence for the sample with use of formulas given in Ref. 20.

magnitude and their influence on the signal intensity cannot be easily separated. In samples with higher Eu^{2+} concentration the skin effect is the dominating mechanism and though one can determine the conductivity from the data[20] the whole information on the source of the free carriers may be lost.

The decisive argument that the Eu^{2+} centers observed in absorption, EPR, and transport measurements are the same centers comes from the analysis of the temperature dependence of the Eu^{2+} EPR signal intensity, $I_{EPR}(T)$, shown in Fig. 7. The data have been corrected for the temperature changes of the Zeeman-level occupation as well as the decrease of the cavity quality factor with increasing temperature.[20] These effects were controlled by the use of a probe sample measured together with the crystal studied. As already mentioned the $I_{EPR}(T)$ dependence is governed both by Eu^{2+} depopulation and by the skin effect. Making use of the information obtained from absorption studies we estimated the number of electrons ionized to the conduction band from Eu^{2+} and hence, taking the typical mobility in CdF_2 (10 $cm^2/V\,s$) and assuming acoustic-phonon scattering, we estimated the sample conductivity $\sigma(T)$. Since in presence of the skin effect the decay of $I_{EPR}(T)$ is a function[20] of $\sqrt{\sigma(T)}$, we were able to estimate the expected changes of $I_{EPR}(T)$ due to the center depopulation and the skin effect. Such a procedure, which is based on the assumption that the sample conductivity is due to Eu^{2+} thermal ionization, allowed us to explain very well the $I_{EPR}(T)$ experimental data. It can be seen that the calculated $I_{EPR}(T)$ dependence (solid line in Fig. 7) follows the $I_{EPR}(T)$ changes. This result is the final verification that Eu^{2+} centers are thermally ionized and that the activation enthalpy of this process is close to 330 meV.

D. Emission and capture processes of the coactivator

The formulas describing the emission and capture processes are well known.[21–23] The relation between the emission (e_n) and capture (c_n) rates is obtained from the detailed balance condition and is given by

$$e_n = X_n c_n N_c \exp\left[-\frac{\Delta H_n}{kT}\right], \tag{4.1}$$

where

$$X_n = \exp\left[\frac{\Delta S_n}{k}\right] \tag{4.2}$$

is the "entropy factor" containing the total change in entropy (due to the change of the vibrational frequency and electronic degeneracy) taking place when electrons are excited from donors to the conduction band. For the polar lattice of CdF_2 the entropy factor cannot be simply partitioned into the vibronic and electronic components. ΔH_n in Eq. (4.1) is the enthalpy needed to emit an electron from the donor to the conduction band, which may be called the activation enthalpy.[24]

The unknown entropy factor is not the only problem encountered in the analysis of emission and capture processes in CdF_2. The concept of the emission and capture rate as defined above has been introduced for standard conduction-band transport and may not apply to the ionic CdF_2 compound. For example, the results of ac conductivity studies[25] may be interpreted by impurity band transport. Furthermore, the carrier mobility in CdF_2 (of the order of 10 $cm^2/V\,s$) is in the range of typical mobilities in amorphous semiconductors.[19] For this reason the experimental results are analyzed in two approaches, one of which is based on formulas (4.1) and (4.2) and leads to the classical Arrhenius plots.

1. Photoexcitation of Eu^{2+} centers. Ionization of the coactivator

It was shown in Secs. IV A and IV B that electrons induced in the conduction band during uv excitation are ionized from the excited states of oxygen and fluorine coactivators, and then captured by isolated Eu^{3+} centers. The kinetics of this process can be studied by measuring the increase of the EPR signal intensity of Eu^{2+}. The reverse process, i.e., the recapture of electrons thermally released from Eu^{2+} traps via the coactivator excited states, is responsible for the thermoluminescence. In this section the former process will be analyzed in detail. The latter will be discussed in Sec. IV D 2.

The uv-light-induced population of the Eu^{2+} states can be described by the following kinetics equations:

$$\frac{d}{dt}N_{(Eu^{2+})} = nc_{Eu}(N_{Eu} - N_{(Eu^{2+})}) - e_{Eu}N_{(Eu^{2+})}, \tag{4.3}$$

$$\frac{d}{dt}n = e_{Eu}N_{(Eu^{2+})} - nc_{Eu}(N_{Eu} - N_{(Eu^{2+})}) + p_{i,X}N_{(X^*)} - nc_X N_{(X^+)}, \tag{4.4}$$

$$\frac{d}{dt}N_{(X^*)} = I\sigma_0(N_X - N_{(X^+)} - N_{(X^*)}) - (p_{i,X} + p_{r,X})N_{(X^*)} + nc_X N_{(X^+)}, \tag{4.5}$$

$$\frac{d}{dt}N_{(X^+)}=p_{i,X}N_{(X^*)}-nc_XN_{(X^+)}\ , \tag{4.6}$$

and

$$N_{(X^+)}=N_{(Eu^{2+})}-(N_{Eu}-N_A)+n\ . \tag{4.7}$$

In the Eqs. (4.3)–(4.7) the following notation is used. N_X is the concentration of F_i^- or O_s^{2-} centers prior to illumination; $N_{(X^*)}$ is the light-induced population of the excited states of F_i^- or O_s^{2-}; $N_{(X^+)}$ is the concentration of the ionized coactivator centers (F_i^0 or O_s^-); I is the light intensity; σ_0 is the optical cross section for intraion excitation of the coactivators; $p_{r,X}$ is the recombination rate of the europium-coactivator pair; $p_{i,X}$ is the ionization rate of the excited state of the coactivator. If the process is thermally activated $p_{i,X}=p'_{i,X}\exp(-E_{b1}/kT)$, where E_{b1} is the effective height of the energy barrier for ionization; c_X is the electron capture rate by ionized coactivators, given by $c_X=c'_X\exp(-E_{b2}/kT)$ when the capture process is thermally activated; E_{b2} is the effective height of the energy barrier for the process; n is the free-electron concentration; N_{Eu} is the total concentration of cubic Eu centers, whereas $N_{(Eu^{2+})}$ is the concentration of Eu^{2+} centers; e_{Eu} is the electron emission rate from Eu^{2+} centers given by Eq. (4.1); c_{Eu} is the electron capture rate by cubic Eu^{3+} centers. For classical conduction-band transport the e_{Eu},c_{Eu},c_X, and $p_{i,X}$ terms are temperature dependent and are equivalent to the discussed above emission and capture rates connected by Eq. (4.1). In the Eqs. (4.3)–(4.7) we assume that the illumination which excites the coactivators does not ionize Eu^{2+} states, which will be confirmed further on.

Before solving Eqs. (4.3)–(4.7) under the equilibrium condition we give a simple description of the Eu^{2+} EPR signal rise after the light is turned on at low temperature. When the temperature is low enough the thermal emission of electrons from Eu^{2+} states can be neglected, moreover, it can be assumed that electrons ionized to the conduction band are primarily captured by Eu^{3+} centers and the term describing their recapture by ionized coactivators can be omitted (the validity of the latter assumption will be proved in the following section). Assuming that the concentrations of excited coactivator states and of photogenerated free electrons reach equilibrium much faster than the concentration of Eu^{2+}

$$\left[\frac{d}{dt}N_{(X^*)}=\frac{d}{dt}n=0\right]\ ,$$

which seems to be justified seeing that the typical increase rate of the Eu^{2+} EPR signal is about $10^{-2}\,s^{-1}$, the initial rise of the Eu^{2+} concentration can be approximated by

$$N_{(Eu^{2+})}(t)-N_{(Eu^{2+})}(0)\cong[N_{Eu}-N_{(Eu^{2+})}(0)]\left[\frac{t}{\tau_i}\right]\ ,$$

where

$$N_{(Eu^{2+})}(0)=N_{Eu}-N_A$$

and

$$\tau_i^{-1}=\frac{I\sigma_0N_Xp_{i,X}}{N_A(p_{r,X}+p_{i,X})}\ . \tag{4.8}$$

The validity of the proposed approximation is confirmed by the observed linear dependence of the increase rate of the Eu^{2+} EPR signal intensity τ_i^{-1} on light intensity I.

According to Eq. (4.8) τ_i^{-1} is proportional to the optical cross section for the coactivators excitation. The spectral dependence of τ_i^{-1} should, therefore, reflect the excitation spectrum of the thermoluminescence. As can be seen in Fig. 2(c) the spectral dependence of the initial increase rate of the Eu^{2+} EPR signal as measured for the CdF_2:Eu 1% sample consists of two superimposed bands which are identical with the excitation bands of the C_{4v} and C_{3v} PL. The third weak band at lower energies indicates that there are some other centers in the sample which can be ionized, however, the process does not lead to Eu^{3+} TL.

Equation (4.8) can be further simplified if we recall that the uv excitation results in a very strong photoluminescence and only a small number of the coactivators is ionized, hence $p_{r,X}\gg p_{i,X}$. Since I, N_X, and N_A are temperature independent, and the temperature dependencies of $p_{r,X}$ and σ_0 should be very weak, the exponential temperature dependence of τ_i (see Fig. 6) indicates that the ionization of the coactivator is temperature activated, $\tau_i^{-1}\propto p_{i,X}=p'_{i,X}\exp(-E_{b1}/kT)$. The activation energy obtained is, therefore, equivalent to the effective height of the energy barrier E_{b1} for the ionization process. However, the magnitudes of the appropriate E_{b1} energies for fluorine and oxygen coactivators are uncertain. If we assume that $p'_{i,X}$ is temperature independent these energies are 13 ± 2 meV for C_{4v} and 56 ± 7 meV for C_{3v} centers, as given in Table II. However, if we consider the classical description of the emission process $p_{i,X}$ is equivalent to the emission rate and then $p'_{i,X}$ depends on temperature as T^2. In such an approach the ionization of C_{4v} centers is not thermally activated, while in the case of C_{3v} centers the E_{b1} energy is reduced to 30 meV.

Equations (4.3)–(4.7) can be solved at the equilibrium condition:

$$\frac{d}{dt}N_{(Eu^{2+})}=\frac{d}{dt}n=\frac{d}{dt}N_{(X^*)}=\frac{d}{dt}N_{(X^+)}=0\ .$$

For low excitation powers, as used in the experiment, the number of excited or ionized coactivators is much smaller than their total concentration, and hence $N_X-N_{(X^*)}-N_{(X^+)}\cong N_X$. Moreover, the light- and temperature-induced concentration of free electrons is small enough to be omitted in the charge neutrality equation (4.7) which can be approximated by $N_{(X^+)}\cong N_{(Eu^{2+})}-(N_{Eu}-N_A)=N_{(Eu^{2+})}-N_{(Eu^{2+})}(0)$. After applying these two approximations to Eqs. (4.3)–(4.7) we obtain

TABLE II. Summarized results of photo-EPR, thermoluminescence, and transport experiments. The activation energies were determined (I) disregarding any temperature dependence of the preexponential factors, (II) assuming standard conduction-band transport.

Activation energy		C_{4v} (meV) I	C_{4v} (meV) II	C_{3v} (meV) I	C_{3v} (meV) II	O_h (meV)
τ_i	E_{b1}	13±2	0	56±7	30	
τ_d	$E_{Eu}+E_{b2}$	352±17	317	450±28	414	
				440±17	407	
TL	$E_{Eu}+E_{b2}$	360±15	335	440±15	415	
I_{EPR}	$E_{Eu}+E_{b2}-E_{b1}$	350±10	350[a]			
σ_{dc}[b]	E_{Eu}					330
σ_{ac}	E_{Eu}					334±9[c]
						326±9[d]
	E_{b1}	13	0	56	30	
	E_{b2}	33[e]	0[f]	110	80	

[a]This result is unaffected by any temperature-dependent preexponential factors whatever the transport mechanism.
[b]Reference 18.
[c]Measured in a CdF_2:Eu sample which contained predominantly C_{4v} centers before annealing in Cd vapor.
[d]Measured in a CdF_2:Eu sample which contained predominantly C_{3v} centers before annealing in Cd vapor.
[e]Obtained from τ_i and I_{EPR} data as more accurate.
[f]This set of values is less consistent than (I), e.g., it follows from the TL activation energy as well as the EPR decay kinetics that $E_{b2}=0$, however, from $I_{EPR}(T)$ we obtain E_{b2} 20 meV.

$$\frac{N_{Eu}-N_{(Eu^{2+})}}{N_{(Eu^{2+})}[N_{(Eu^{2+})}-N_{(Eu^{2+})}(0)]}=\frac{C}{I}\exp\left[-\frac{E_{Eu}+E_{b2}-E_{b1}}{kT}\right], \quad (4.9)$$

where C is given by

$$C=\frac{e'_{Eu}c'_X p_{r,X}}{\sigma_0 N_X p'_{i,X} c'_{Eu}} \quad (4.10)$$

and is temperature dependent (if we disregard the weak temperature dependencies of σ_0 and $p_{r,X}$) even for standard conduction-band transport. In (4.9) E_{Eu} is the activation enthalpy of Eu^{2+}, denoted as ΔH_n in Eq. (4.1).

The temperature and light-intensity dependencies of the saturation amplitude of the Eu^{2+} EPR signal under illumination from the C_{4v} excitation region are shown in Fig. 8. The activation energy obtained from the fit of the temperature dependence with formula (4.9) is $(E_{Eu}+E_{b2}-E_{b1})=350\pm10$ meV. The fitting parameters found to be the best for the description of the temperature dependence were then used to calculate the light-intensity dependence. The very good agreement of the experimental and calculated values [shown in Fig. 8(b)] confirms the applicability of formula (4.9) to the description of the experimental results. The above-discussed experiment can provide the decisive argument for the existence of the E_{b1} energy barrier in the case of C_{4v} centers. As the activation energy governing the temperature dependence of the saturation amplitude is equal to $E_{Eu}+E_{b2}-E_{b1}$, by comparing it to the activation energy derived from the thermoluminescence studies (which in our notation is given by $E_{Eu}+E_{b2}$) the value of E_{b1} can be determined. The $E_{Eu}+E_{b2}$ energy can be also established independently from the kinetics of the Eu^{2+} EPR signal decay after the light is turned off. Therefore, before further discussion of the activation character of the coactivators ionization processes the capture process will be described.

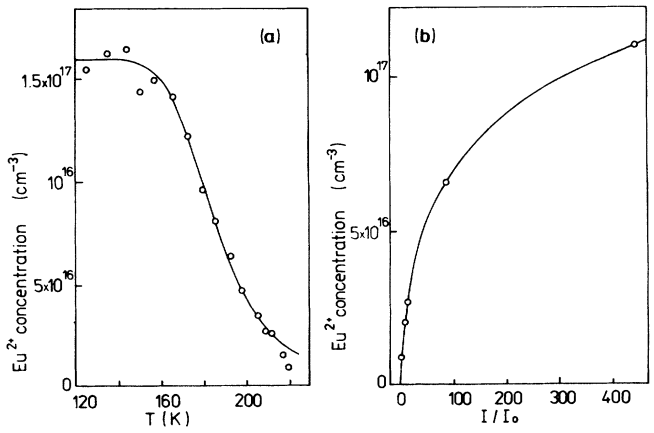

FIG. 8. (a) Temperature and (b) light-intensity dependencies of the saturation amplitude of the Eu^{2+} EPR signal observed under 333-nm illumination. The lines represent the fit to the data with use of Eqs. (4.9) and (4.10) for the following parameters: $E_{Eu}+E_{b2}-E_{b1}=354$ meV; $C/I=1.08\times10^{-7}$ cm^3. The light-intensity scale in (b) is a relative one, $I=440I_0$ is the intensity applied in (a).

2. *The kinetics of the thermoluminescence process*

The results discussed in the preceding sections prove that during uv excitation electrons are ionized from F_i^- and O_s^{2-} coactivators of the C_{4v} and C_{3v} PL, and captured by cubic Eu^{3+} centers. We propose that the reverse process, i.e., the recapture of electrons thermally released from the populated Eu^{2+} centers by the ionized coactivators, proceeds via the coactivator excited states. The subsequent deexcitation within the C_{4v} and C_{3v} centers results in the observed TL emission. Such a model of the thermoluminescence process we base on the fact that (i) the TL emission is similar to the photoluminescence hence the radiative deexcitation is analogous (see Fig. 1); (ii) the temperature range in which the depopulation of the light-induced Eu^{2+} centers is observed is correlated with the range in which thermoluminescence occurs (Figs. 4 and 8).

In consequence, the decay of the Eu^{2+} EPR signal after the light is turned off should monitor directly the kinetics of the thermoluminescence process. The appropriate kinetics equations can be derived from Eqs. (4.3)–(4.6) by omitting the excitation term $I\sigma_0(N_X - N_{(X^*)} - N_{(X^+)})$. Moreover, since $p_{r,X} \gg p_{i,X}$ most of the electrons captured by the coactivators on their excited states recombine immediately within the oxygen-europium or fluorine-europium pairs and the ionization term $N_{(X^*)}p_{i,X}$ can be omitted as well. We utilize also the $N_{(X^+)} \cong N_{(Eu^{2+})} - (N_{Eu} - N_A)$ approximation used in Sec. IV D 1. A further simplification results from the fact that in the temperature range in which the decay of the Eu^{2+} EPR signal is observed the light-induced concentration of Eu^{2+} is much smaller than $(N_{Eu} - N_A)$ and, consequently, the free-electron concentration is dominated by its equilibrium value: $n \approx e_{Eu}(N_{Eu} - N_A)/(c_{Eu}N_A)$. The solution is then easily found and takes the simple exponential form:

$$N_{(Eu^{2+})} - (N_{Eu} - N_A) = [N_{(Eu^{2+})}(0) - (N_{Eu} - N_A)] \exp(-t/\tau_d) ,$$

where

$$\tau_d = \frac{c_{Eu}N_A}{c_X e_{Eu}(N_{Eu} - N_A)} = \frac{c_{Eu}N_A}{c'_X e'_{Eu}(N_{Eu} - N_A)} \exp\left[\frac{E_{Eu} + E_{b2}}{kT}\right] . \quad (4.11)$$

Here $N_{(Eu^{2+})}(0)$ is the Eu^{2+} concentration at the moment when the light is turned off, and E_{Eu} denotes the activation enthalpy ΔH_n in Eq. (4.1). As can be seen the decay time τ_d depends exponentially on temperature, however, in the "classical" description the T^2 preexponential factor should be taken into account.

The decay kinetics of the Eu^{2+} EPR signal intensity after the light was turned off was measured in the temperature range 180–230 K. Since the concentration of light-induced Eu^{2+} centers decreases with increasing temperature (see Fig. 8) in the experiment an efficient broadband illumination was applied. The kinetics of the EPR signal decay was found to be described by a sum of two exponential functions. The temperature dependencies of the decay time constants for the fast and slow components of the decay [shown in Fig. 4(b)] are distinctly different and yield the activation energies of 451±28 and 352±17 meV, respectively. These energies are similar to those found in thermoluminescence experiments for C_{3v} (440±15 meV) and C_{4v} (360±15 meV) emissions. Therefore, we propose that the fast and slow components of the decay relate to the capture of electrons thermally released from Eu^{2+} traps on two different kinds of centers: the O_s^- ionized coactivator in the C_{3v} center and F_i^0 in the C_{4v} center, respectively. Such a capture process involving two centers is possible since the broadband uv illumination employed in the discussed experiment ionized both C_{4v} and C_{3v} centers. The different decay rates of the two capture processes are a direct consequence of the fact that τ_d^{-1} is proportional to the electron capture rate of the coactivator. Hence, the ratio of the capture rates by the ionized oxygen and fluorine coactivators, $c'_{(O^-)}/c'_{(F^0)}$, can be estimated and is found to be of the order of 2×10^3. This value also gives the ratio of the capture cross sections, σ, independent of the transport mechanism in CdF_2. To determine their absolute magnitudes, however, some assumptions are required. If we take the entropy factor[26] as 18±2 we obtain $\sigma_{(O^-)} \approx 10^{-18}$ cm^2. This seems to be rather small for an electron attractive center.

The above-mentioned two components of the Eu^{2+} EPR signal decay will be observed only in crystals in which both types of Eu^{3+} complexes are present and their concentrations are similar. For example, in the previous studies of von Bardeleben[27] only the slow component of the decay was observed. The hypothesis that the fast and slow components in the decay of Eu^{2+} are connected with electron capture by O_s^- and F_i^0 coactivators is verified by the experiment in which the 254-nm excitation was applied. This excitation ionizes primarily the C_{3v} centers. Indeed, only one type of center was found to be active in the capture process and the activation energy obtained from the plot of $\ln\tau_d$ vs $10^3/T$ shown in Fig. 4(b) (440±17 meV) agrees very well with the activation energy for capture by C_{3v} centers [see the bottom of Fig. 4(a)].

E. The model of the thermoluminescence process

The experimental results discussed in Sec. IV D are summarized in Table II. Because of the unknown transport mechanism in the CdF_2 lattice it is not clear how to determine properly the activation energies from the experimental data. Therefore, in Table II two sets of activation energies are given—the first one obtained assuming temperature-independent emission and capture rates (apart from the exponential dependence) and the second obtained assuming standard conduction-band transport [with the capture and emission rates related via the detailed balance equation (4.1)]. Though the validity of the latter description cannot be formally excluded, the first

set of data seems to be more consistent. For example, the $(E_{Eu}+E_{b2})$ energies established from the decay kinetics of the Eu^{2+} EPR signal agree in that approach with the activation energies obtained from thermoluminescence data, which in our notation should also be equal to $(E_{Eu}+E_{b2})$. Furthermore, the activation energy $(E_{Eu}+E_{b2}-E_{b1})$ determined from the saturation amplitude of the Eu^{2+} EPR signal $[I_{EPR}(T)]$ under illumination which ionizes C_{4v} centers agrees with other data only for E_{b1} and E_{b2} energies taken from the first set of the data. Moreover, the E_{b2} energy agrees very well with the 32-meV activation energy obtained from thermostimulated current studies by de Murcia *et al.*[10] and interpreted as the effective height of the energy barrier for electron capture by the fluorine coactivator.

The logical consequence of our supposition that the transport mechanism in CdF_2 is not a pure conduction band one is the possibility of electron diffusion between the Eu^{2+} trap and the Eu^{3+}-O_s^- and Eu^{3+}-F_i^0 complexes being thermally activated. If such an activation energy (E_{diff}) exists it will affect all the activation energies obtained from kinetics experiments. For example, the increase kinetics should be governed by the $E_{b1}+E_{diff}$ energy instead of E_{b1}. As can be seen in Table II the upper limit of E_{diff} is 13 meV, i.e., the energy obtained from the Eu^{2+} increase rate for C_{4v} center ionization. It seems that if the diffusion activation energy were not negligible a difference in the activation energies for dc and ac transport should be expected (as in dc transport the highest resistivity paths decide about the conductivity magnitude, whereas in the case of ac measurements the low resistivity paths are dominating). However, the temperature dependencies of ac conductivity measured for two types of CdF_2:Eu crystals (one containing mainly C_{4v} centers and the other C_{3v} centers before thermal conversion) yield the activation energies of 334±9 and 326±9 meV, respectively (Fig. 9), which agree (within the experimental error) with the 330-meV activation energy of dc transport established by Trautweiler, Moser, and Khosla.[18] We can, therefore, assume that if the E_{diff} energy exists, it is fairly small and should not disturb appreciably the energies given in Table II.

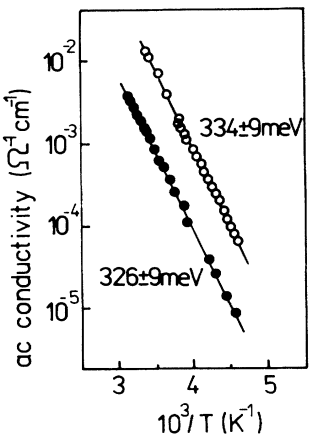

FIG. 9. Temperature dependence of ac conductivity measured in two thermally converted CdF_2:Eu samples containing mainly C_{3v} (full circles) and C_{4v} (open circles) centers before the conversion process.

Up to now we have disregarded the possibility that the electron capture by cubic Eu^{3+} centers may be also thermally activated. The existence of an energy barrier for the process $(E_{b(Eu)})$ should be the more carefully verified since such a barrier is known to occur in the case of the indium impurity in CdF_2. Moreover, this barrier is responsible for the population inversion between In^{2+} localized and $In^{3+}+e^-$ hydrogeniclike donor states.[28] In order to verify the presence of the $E_{b(Eu)}$ energy barrier the following experiment was performed. A converted CdF_2:Eu sample, containing only Eu^{2+} centers was illuminated with light inducing the $4f^7 \rightarrow 4f^6 5d^1$-allowed transition of Eu^{2+}. This illumination was shown previously[11] to lead to a very effective ionization of Eu^{2+} centers, which can be observed as a quenching of the Eu^{2+} EPR signal in crystals with other than Eu trap centers present. In the converted crystal, however, the electrons induced in the conduction band were found to be immediately recaptured by Eu centers and no Eu^{2+} photoquenching was observed, even at 4.2 K. This allows us to conclude that there is no significant energy barrier for the capture of electrons by Eu centers.

Though the values given in Table II should be considered only as the upper limits of the effective barrier heights (resulting from the competition between the thermally activated transition over the barrier and tunneling), for further discussion it is pertinent that for both types of centers (C_{4v}, C_{3v}) the E_{b2} barrier is higher than E_{b1}. It means that the activation energy for carrier capture is larger than the appropriate energy for its thermal release. It can be readily shown that such a situation occurs only when the excited states of the coactivators are degenerate with the continuum of conduction-band states. The carrier emission process is, in fact, an autoionization process. Its activation character is due to the lattice-relaxation-induced energy barrier which separates the excited and ionized states of the coactivator. This is schematically shown in Fig. 10(a). The model shown in this figure also allows us to explain the thermally activated character of the capture process (governed by the E_{b2} barrier). It is clear that the activation energy determined from either TL or photo-EPR decay studies is larger than the Eu^{2+} activation enthalpy (E_{Eu}) and equal to $E_{Eu}+E_{b2}$.

In the model shown in Fig. 10(a) we assume that the excited state from which the electrons are ionized and on which they are captured is the same. However, previous luminescence studies of one of the authors[3] suggest that in the case of the oxygen coactivator a different situation is possible. While the excitation process (at 4.8 eV) was shown to be due to the $^1S_0(2p^6) \rightarrow {}^1P_1(2p^5 3s^1)$ transition of O_s^{2-}, the energy transfer to Eu^{3+} was suggested to occur from the lower triplet state $^3P_J(2p^5 3s^1)$. Since the $^3P_J \rightarrow {}^1S_0$ transition is forbidden, energy transfer to the Eu^{3+} center can be more efficient than direct radiative deexcitation. In fact, the $^3P_J \rightarrow {}^1S_0$ emission of oxygen (at 2.7 eV) is only observed for oxygen-rich CdF_2 crystals

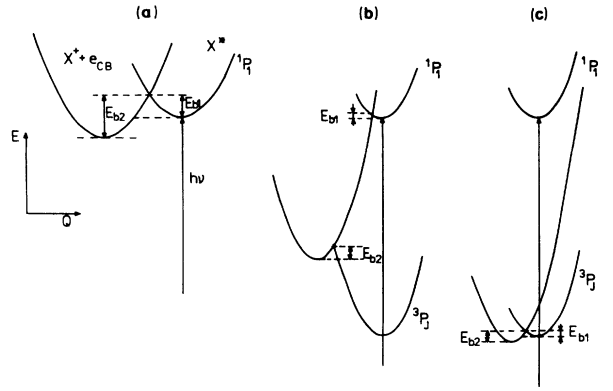

FIG. 10. The configuration coordinate diagram of the position of the coactivator excited states with respect to the conduction band for the following cases: (a) The barriers for autoionization E_{b1} and capture E_{b2} relate to the $^1P_1$ excited state of the coactivator; (b) the E_{b1} barrier is connected with the $^1P_1$ state, but the E_{b2} barrier occurs at the ^3P_J state; (c) both barriers relate to the ^3P_J state.

not codoped with europium. In consequence, we should distinguish among three possible situations: when the E_{b1} and E_{b2} barriers relate to the $^1P_1$ state [Fig. 10(a)]; the E_{b1} barrier is connected with the $^1P_1$ state, but the E_{b2} barrier occurs at the ^3P_J state [Fig. 10(b)]; both barriers relate to the ^3P_J state [Fig. 10(c)].

It is evident that in the last case a broad photoionizatoin band should be observed starting at an energy lower than that of the $^1S_0 \rightarrow {}^1P_1$ transition of O_s^{2-}. Since in the TL excitation spectrum such a band has not been observed this case can be immediately rejected. The experimental results do not allow, however, to distinguish between the other two cases. It is only certain that the $^1P_1$ state undergoes autoionization. As the location of this state in respect to the conduction-band edge is unknown we cannot exclude the possibility that in the capture process the ^3P_J state of the oxygen coactivator is active. The situation for the fluorine coactivator is more clear. No emission suggesting that the energy transfer might proceed from the ^3P_J state has been observed for isolated F_i^- ions. Moreover, the studies of mixed $Cd_{1-x}Ca_xF_2$:Eu crystals[29] indicate that both the autoionization and capture processes most probably involve only the $^1P_1$ state of F_i^-. By analogy, we propose that the same [the model shown in Fig. 10(a)] occurs also for the oxygen coactivator, but this cannot be considered as a proven fact.

V. CONCLUSIONS

The model presented in Figs. 10(a) and 10(b) allows us to explain all the features of the complex thermoluminescence process in the CdF_2:Eu lattice. It is shown that two types of europium centers are active in this process: the charge-compensated Eu^{3+}-O_s^{2-} or Eu^{3+}-F_i^- associates (the centers which dominate the photoluminescence under broadband uv excitation), and the cubic Eu^{3+} centers without any close charge compensation (which are the electron traps). The presence of cubic centers is necessary for the thermoluminescence to occur and their concentration controls the intensity of this process. The Eu^{3+}-O_s^{2-} (C_{3v} symmetry) and Eu^{3+}-F_i^- (C_{4v} symmetry) centers play a double role. First of all they are a source of electrons due to the autoionization of their excited states. On the other hand, the electrons thermally released from Eu^{2+} donors are retrapped by the O_s^- and F_i^0 ionized coactivators in the C_{3v} and C_{4v} complexes. The deexcitation process within the oxygen-europium and fluorine-europium centers is identical to the one governing the photoluminescence. It means that the energy of the coactivator, which is in the excited state after electron capture, is transferred to Eu^{3+}, and then Eu^{3+} radiative recombination follows. Therefore, the emission spectra in the PL and TL processes are identical, as well as their excitation spectra.

The CdF_2 thermoluminescence is a good example of demonstrating the role of lattice relaxation in electronic transitions. The existence of an energy barrier for the autoionization process explains two of the strange features of the CdF_2:Eu thermoluminescence: the fact that the excitation spectra of the PL and TL processes are the same, and that the autoionization process is thermally activated. On the other hand, the lattice-relaxation-induced energy barrier for the capture process explains another puzzle encountered when studying CdF_2:Eu TL, i.e., the spread of the activation energies established from the thermoluminescence studies. They were different for different emitting centers and larger than Eu^{2+} activation enthalpy. This suggested that the electrons might be captured by Eu^{3+} ions within the various associates as the close-lying coactivator could affect the activation enthalpy of such Eu^{2+} traps. We reject such a model of the thermoluminescence on the basis of very detailed photo-EPR studies. It is unambiguously shown that the spread of the TL activation energies is due to the presence of energy barriers for the electron capture process.

The fact that the experimental data are more consistently described when we neglect the temperature corrections resulting from the "classical" conduction-band transport description seems to indicate that the transport mechanism in CdF_2 might not be a standard conduction-band one, as observed in less ionic crystals. The problem of an appropriate description of the CdF_2 transport cannot be, however, solved on the basis of the presented studies and further investigations are necessary.

ACKNOWLEDGMENTS

The authors wish to thank Professor J. M. Langer for helpful discussions and T. Langer for preparing the samples.

[1]R. L. Calvert and R. J. Danby, Phys. Status Solidi A **83**, 597 (1984).
[2]D. Hommel, J. M. Langer, and B. Krukowska-Fulde, Phys. Status Solidi A **31**, K81 (1975).
[3]D. Hommel and J. M. Langer, J. Lumin. **18/19**, 281 (1979).
[4]J. P. Jouart, C. Bissieux, M. Egee, G. Mary, and M. de Murcia, J. Phys. C **14**, 4923 (1981).
[5]Sun-Il Mho and J. C. Wright, J. Phys. Chem. **77**, 1183 (1982).
[6]P. F. Weller, Inorg. Chem. **4**, 1545 (1965).
[7]S. Benci and G. Schianchi, J. Lumin. **11**, 349 (1976).
[8]E. Banks and R. W. Schwartz, J. Chem. Phys. **51**, 1956 (1969).
[9]M. J. Vrabel and H. A. Atwater, J. Chem. Phys. **48**, 946 (1968).
[10]M. de Murcia, Jin Yixin, P. Bräunlich, J. P. Jouart, and H. J. von Bardeleben, J. Phys. C **15**, 2069 (1982).
[11]M. Godlewski, D. Hommel, J. M. Langer, and H. Przybylinska, J. Lumin. **24/25**, 217 (1981).
[12]D. Hommel, Ph.D. thesis, Institute of Experimental Physics, Warsaw University, Warsaw, 1979.
[13]H. J. Gläser and D. Geist, Z. Naturforsch. Teil A **23**, 1980 (1968).
[14]D. Geist, E. Gerstenhauser, and G. Rackebrandt, Z. Naturforsch. Teil A **26**, 1589 (1971).
[15]T. Rewaj and M. Krupski, Phys. Status Solidi B **99**, 285 (1980).
[16]K. Baberschke, Z. Physik **252**, 65 (1972).
[17]R. Lacroix, Helv. Phys. Acta **30**, 374 (1967).
[18]F. Trautweiler, F. Moser, and R. P. Khosla, J. Phys. Chem. Solids **29**, 1869 (1968).
[19]N. F. Mott and E. A. Davis, in *Electronic Processes in Non-crystalline Materials* (Clarendon, Oxford, 1971).
[20]M. Godlewski, H. Przybylinska, and J. M. Langer, Appl. Phys. A **30**, 105 (1983).
[21]O. Engström and A. Alm, J. Appl. Phys. **54**, 5240 (1983); Solid State Electronics **21**, 1571 (1978).
[22]R. N. Hall, Phys. Rev. **87**, 387 (1952).
[23]W. Shockley and W. T. Read, Phys. Rev. **87**, 835 (1952).
[24]D. V. Lang, H. G. Grimmeiss, E. Meijer, and M. Jaros, Phys. Rev. B **22**, 3917 (1980).
[25]E. Loh, Phys. Rev. **175**, 533 (1968).
[26]H. Przybylinska and M. Godlewski (unpublished).
[27]H. J. von Bardeleben, J. Phys. C **17**, 2391 (1984).
[28]U. Piekara, J. M. Langer, and B. Krukowska-Fulde, Solid State Commun. **23**, 583 (1977).
[29]H. Przybylinska and M. Godlewski (unpublished).